Urban Forestry & Urban Greening 101 (2024) 128495



Contents lists available at ScienceDirect

Urban Forestry & Urban Greening

journal homepage: www.elsevier.com/locate/ufug



Toward carbon neutral cities: A comparative analysis between Sentinel 2 and WorldView 3 satellite image processing for tree carbon stock mapping in Brussels

MD Abdul Mueed Choudhury [a,*], Ernesto Marcheggiani [a,b,**], Giuseppe Modica [c], Salvatore Praticò [d], Ben Somers [b]

[a] Department of Agricultural, Food and Environmental Sciences, Marche Polytechnic University, Italy
[b] Division of Forest, Nature and Landscape, Department of Earth and Environmental Sciences, KU Leuven, Leuven 3001, Belgium
[c] Department of Veterinary Sciences, University of Messina, Italy
[d] Department of Agriculture, Mediterranean University of Reggio Calabria, Italy

ARTICLE INFO

Handling Editor: Dr Cecil Konijnendijk van den Bosch

Keywords:
Urban trees and Urban forests
Carbon stock (CS)
Sentinel 2 data
WorldView 3
NDVI (Normalized Difference Vegetation Index)
Carbon neutral cities

ABSTRACT

Because of the high costs associated with data sources, urban policymakers struggle to employ cost-effective remote sensing methods for evaluating trees and their potential contributions to atmospheric Carbon Stock (CS). While free data sources like Copernicus Sentinel satellite data could be explored, there are a few studies illustrating its potential for mapping urban tree C. Here, the Sentinel 2 (S2)-derived Normalized Difference Vegetation Index (NDVI) was used to model CS for street trees in Brussels. In parallel, the WorldView 3 (WV3)-derived NDVI layer was also used for a similar study area to compare the CS mapping outcomes regarding dominant tree species. The accuracy level was around 90 % (R^2=0.89, r=0.94, and RMSE= 97 kg) in the case of WV3 data, whereas it was about 60 % (R^2=0.60, r=0.79, and RMSE = 189.6 kg), even with a coarse resolution regarding the S2 data. This study also shows the strength and scope of using S2 data over WV3 data, illustrating the convenience in terms of accuracy and cost-effectiveness compared to existing methods. The applied methodology could be utilized to monitor urban trees and predict the level of possible carbon sequestration, even considering a larger city like Brussels with a complex agglomeration. It could be a solid additional support for the authorities of European towns and developing countries, especially in terms of being cost-efficient and readily embraced by users.

1. Introduction

Urban green networks and trees have become well-recognized as a practical tool for mitigating the worsening impacts of ceaseless carbon emissions. Big cities, covering only 1 % of the planet, are responsible for exhaling about 80 % of the globally emitted CO_2 (Lechtenböhmer et al., 2009; OPUS 4). Trees could undoubtedly play a considerable role by trapping and stocking atmospheric carbon, in other ways known as carbon sequestration. For instance, it has been suggested that the total yearly reduction in carbon emission can be up to 18 kg/tree in urban areas (Kanniah et al., 2014; Rosenfeld et al., 1998). It is evident that urban trees can provide a solid way to reduce carbon emissions (Sahle et al., 2018; Gülçin and Konijnendijk Van Den Bosch, 2021; Qin et al., 2022; Choudhury et al., 2021, 2020), which also recognizes trees and their contribution to a city's climate towards the goal of carbon neutrality. When quantifying the possible tree-stand Carbon Stock (CS), existing tree species information and imputations of the inventory-based analysis are essential to city planners. Tree-stand aerial CS is one of the critical features of the urban ecosystem, either for enriching air quality or concerning a carbon-neutral environment. It is essential to understand the applicability of the tree inventory-based CS imputation approaches, especially to decelerate the impacts of disappearing green spaces due to rapid urbanization. Over the last few decades, urban trees and their possible CS potentialities have been recognized and assessed in

* Corresponding author.
** Corresponding author at: Department of Agricultural, Food and Environmental Sciences, Marche Polytechnic University, Italy.
E-mail addresses: m.choudhury@staff.univpm.it (M.A.M. Choudhury), e.marcheggiani@staff.univpm.it, ernesto.marcheggiani@kuleuven.be (E. Marcheggiani), giuseppe.modica@unime.it (G. Modica), salvatore.pratico@unirc.it (S. Praticò), ben.somers@kuleuven.be (B. Somers).

https://doi.org/10.1016/j.ufug.2024.128495
Received 17 November 2023; Received in revised form 23 June 2024; Accepted 25 August 2024
Available online 31 August 2024
1618-8667/© 2024 The Author(s). Published by Elsevier GmbH. This is an open access article under the CC BY license (http://creativecommons.org/licenses/by/4.0/).

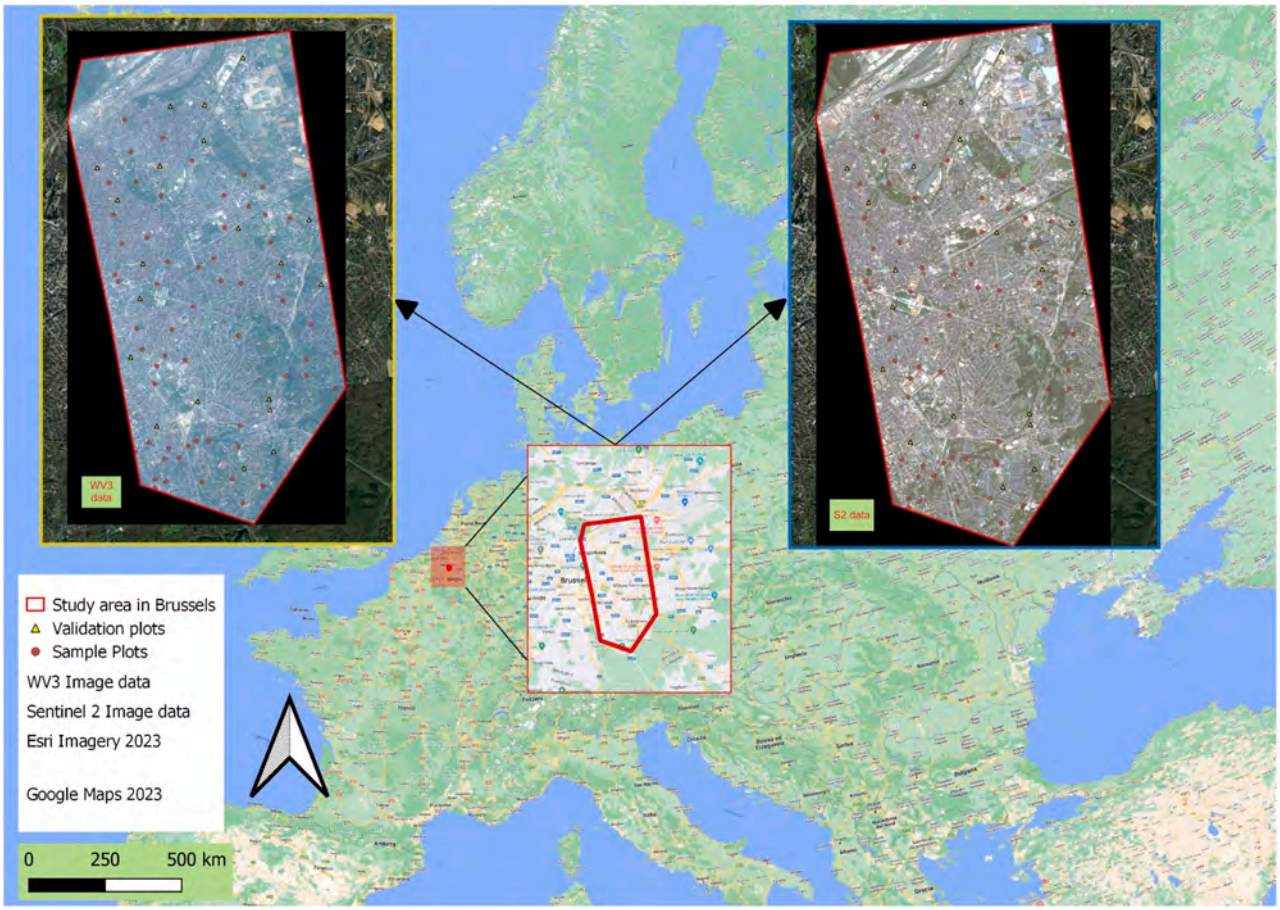

Fig. 1. The Sentinel-2 (S2) and WorldView-3 (WV3) data of the study area, including the sample and validation plots in Brussels.

many studies, from manual tree by tree to the most updated remote-sensing approaches (Li et al., 2019; Song et al., 2016; Myeong et al., 2006; Feng et al., 2016; Wei et al., 2022). However, most approaches are hardly accessible to the city authorities because of the overpaid data sources and their postprocessing complications. Several studies also used different approaches to quantify tree CS or dry biomass utilizing LiDAR data or other commercially available data integrated with LiDAR for better accuracy (Qin et al., 2022; Wilkes et al., 2018; Mariappan et al., 2012; Zhang and Shao, 2021). These studies have mostly been done for an urban park or a smaller study area, which does not recognize their applicability either regarding a more extensive study area or concerning cost-effective prospects.

To track and monitor tree-stand CS in city areas, updating accurate information on tree inventories is crucial to the city authorities. Traditionally, urban tree studies have commonly relied on methods based on random field sampling and interpreting aerial photographs, which tend to be costly, require a significant amount of labor, and are time-consuming interest (Li et al., 2019; Song et al., 2016; Myeong et al., 2006; Pu, 2011). However, research on urban tree characteristics, including their identification, categorization, and the mapping of CS, encounters difficulties due to the adoption of complicated and multi-faceted techniques and a scarcity of pertinent data information (Li et al., 2019; Tigges and Lakes, 2017). Lately, remote-sensing approaches based on field surveys have been applied to calibrate the tree dendrometry, i.e., Diameter at Breast Height (DBH) and Height (H) in urban areas (Panagiotidis et al., 2016a; Yao et al., 2012; Panagiotidis et al., 2016b). However, species-specific Above Ground Biomass (AGB) estimation methods for urban trees remain limited due to the intricate nature of urban agglomerations, including variations in land cover, frequent shaded areas caused by buildings and trees, and the intricate composition of urban forests in contrast to natural and planted forests. LiDAR data are being highly recognized, either terrestrial or airborne, to estimate biomass and carbon storage in urban vegetation (Mitchell et al., 2018; Shrestha and Wynne, 2012; Raciti et al., 2014; Alonzo et al., 2016), but it is still expensive and hardly cost-effective for the public authorities. Exploring potential multispectral data, i.e., Sentinel-2 (S2) and WorldView-3 (WV3) data, could alter the solution, especially in terms of convenience and applicability concerning a typical urban surface. Previous studies showed the diversified applications of commercially available data sources like WV3 (He et al., 2020; Fassnacht et al., 2016; Johnson and Jozdani, 2018; Degerickx et al., 2020; Puissant et al., 2014; Pu and Landry, 2020, 2012; Solano et al., 2019), freely accessible S2 data could be utilized more to understand its applicability than other data sources.

There is now a growing need to introduce a cost-effective and convenient approach, particularly for urban policymakers. Concerning the existing issues, the main goal of this study was to recommend a cost-effective species-based urban tree CS estimation and mapping approach comparing the commercial WV3 image data with the free S2 data. This approach has been applied considering three specific steps: (1) Estimation of the CS/plot utilizing tree allometry; (2) utilizing tree information shapefile for the species-based CS mapping; (3) comparing the WV3 data with the S2 data concerning the city-wide CS imputations. This study also illustrates the convenience of this mapping approach even for updating tree inventory-based information in regular intervals, which could be strongly applicable for urban planners towards a sustainable strategy focusing on the goal of carbon neutrality.

Table 1
The table shows the details of the remote sensing data utilized in this study.

Data	Description
WorldView 3 (WV3) [8 multispectral bands+1 panchromatic band]	• Acquisition date: April 2017 • Resolution: 1.2 m • Available on: http://worldview3.digitalglobe.com/
Sentinel 2 [13 Spectral bands]	• Acquisition date: January to August 2022 • Resolution: 10–60 m • Available on: https://dataspace.copernicus.eu/

2. Materials and methods

2.1. Dataset

The tree data were collected in Brussels, the European capital region situated precisely in the Northwestern part of the continent (50°50′N 4°00′E) (Fig. 1). Earlier in February 2022, the field plots were randomly selected, covering a study area of around 49 km^2, where a total number of 80 plots has been surveyed. Tree species information and the DBH, the H, and plot-level coordinates have been recorded for each plot. Each plot covered an area of (10 m×10 m) 100 m^2, where 20 out of 80 plots were used as the reference plots for validation. Three different types of species, i.e., *Acer spp., Tilia spp., and Aesculus hippocastanum,* have been identified, while the number of trees occupying each plot was precisely more than 2(in an average of 2–4)of the same species. An allometric model (Tabacchi et al., 2011a) has been utilized to estimate AGB per plot, leading to the imputations of the species-based CS for the whole study area.

S2 and the WV3 image data have been utilized to predict and map the species-based CS in Brussels [Fig. 1]. Starting from January to August 2022, 20 different S2 images were downloaded with a least possible cloud cover of around 15 % using the Semi-Automatic Classification Plugin (SCP) (Congedo Luca) in QGIS (Table 1). The S2 data comprises 13 spectral bands covering the visible and near- to short-wave infrared spectrum, with pixel sizes ranging from 10 to 60 m, freely available on the Copernicus hub, generated by the European Space Agency (ESA) since 2014. The WV3 is a high-resolution commercial Earth observation satellite operated by DigitalGlobe (Table 1), launched on August 13, 2014. The WV3 imagery is well known for its higher geolocation accuracy, with a panchromatic band of up to 0.3 m ground sample distance (GSD) and eight other multispectral bands with 1.2 m GSD. To compare the results with the S2 data, a WV3 image acquired in April 2017 was utilized from a previous study (Choudhury et al., 2021).

2.2. Methods

Concerning the species-based CS estimation, tree dendrometric information, i.e., DBH and H, were collected for all trees within each plot during the field survey. This study measured tree H using the Nikon Forestry 550, a laser rangefinder designed explicitly for forestry use, equipped with angle compensation technology (Nikon). A tap measure has taken the stem circumference at 1.3 m from the ground. Later, DBH was calibrated based on the circumference of each of the trees. An allometric model for the European species developed by Tabacchi et al. in 2011 (Tabacchi et al., 2011b) has been used to estimate the AGB for each tree species. This model utilizes H and DBH information to estimate the tree stand AGB (Tabacchi et al., 2011a). Here, the estimated H and

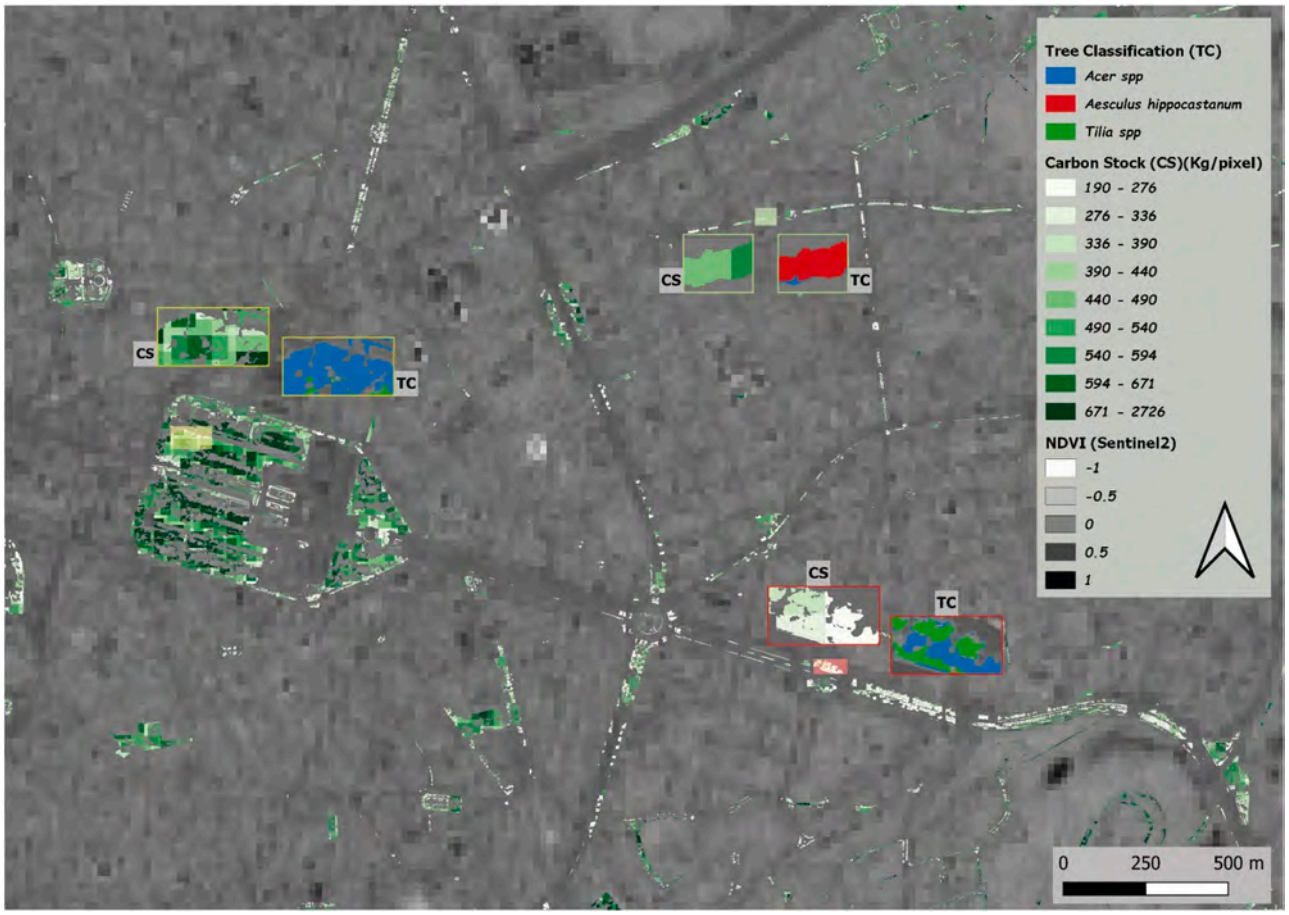

Fig. 2. The species-based Carbon Stock (CS) distribution on Sentinel 2 (S2) image data (NDVI) across the study area in Brussels.

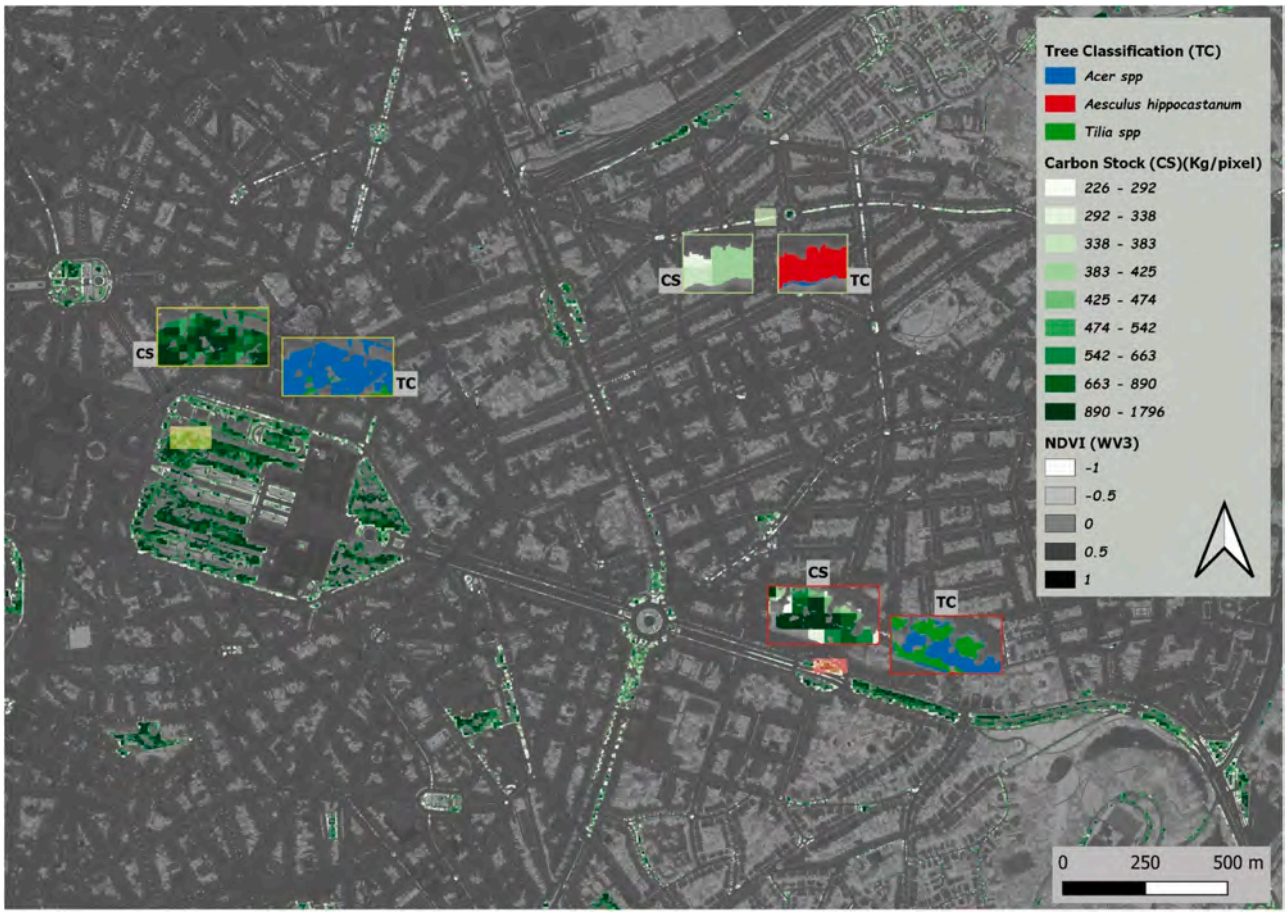

Fig. 3. The species-based Carbon Stock (CS) distribution on WV3 image data (NDVI) across the study area in Brussels.



Fig. 4. Linear correlation of NDVI-based CS (kg per plot) versus estimated CS (kg per plot) on the validation plots.

DBH have been considered to calibrate the mean AGB per plot based on the allometric model (Tabacchi et al., 2011b). As the tree above ground CS has been recommended to be 50 % of the total AGB (Goslee et al., 2010; $author1$ et al., 1986; Losi et al., 2003; Vashum and Jayakumar, 2012; Whittaker and GE., 1973), the mean CS per plot was calibrated by multiplying the mean AGB per plot by 0.5 as a conversion factor (Statistics, 2010; Vicharnakorn et al., 2014a; Panel, 2007).

Later, the S2 images were preprocessed in the SCP plugin (Congedo), using the 'band stacking' module (Congedo, 2016, 2021) within the QGIS environment. The resultant image data, as shown in Fig. 1, were then saved as raster data to introduce the computation of the normalized vegetation difference index (NDVI) (Choudhury et al., 2021, 2020; Shafizadeh-Moghadam et al., 2022; Hird and McDermid, 2009; Baniya et al., 2018). Following this, the 'Zonal statistics' (Jung, 2013) plugin has been utilized to extract CS values for each pixel across the entire study area (Choudhury et al., 2021, 2020).

In the case of WV3 image data, the NDVI layer was computed and used in 'Zonal statistics' to extract pixel-based CS values for each identified species. In both cases of S2 and WV3 data, 60 out of the 80 sample plots were considered, excluding the validation plots.

A shapefile of the identified tree species was required to map the computed CS for the tree species in the study area (Choudhury et al., 2021, 2020). The WV3 image data has been utilized to run the tree classification following the recommended Object-Based Image Analysis (OBIA) procedure on the Trimble eCognition Developer® 10.2 platform (Trimble, Munich, Germany) (AG., 2005) (more details are reported in previous articles of the research group (Choudhury et al., 2021), 2020). The classified tree shapefile of all three identified tree species, i.e., *Acer spp., Tilia spp.,* and *Aesculus hippocastanum,* was then exported to QGIS for further illustrations. Based on the tree species classification shapefile, a fishnet with a 100 m^2 (10 m × 10 m) resolution was constructed to illustrate the CS zones with minimum to maximum values. This

Table 2
The table shows the regression analysis results for the validation plots.

Tree species	Mean CS from field estimation(kg/plot)	CS in QGIS computation on (NDVI) WV3 data (kg/plot)	CS in QGIS computation on (NDVI) Sentinel2 data (kg/plot)	Regression analysis			
				WV3 data (NDVI) and field-estimated CS	Sentinel2 data (NDVI) and field-estimated CS	The overall coefficient of determination for all the validation plots	
						WV3 data (NDVI) and field-estimated CS	Sentinel2 data (NDVI) and field-estimated CS
Tilia spp.	88	266	292	$R^2 = 0.84$	$R^2 = 0.79$	**$R^2 = 0.89$ ($y = 0.8862x - 14.198$) r =0.94 RMSE = 97 kg**	**$R^2 = 0.60$ ($y = 1.0001x - 0.0589$) r =0.79 RMSE = 189.6 kg**
	125	182	311				
	236	142	301				
	302	189.7	236				
	627	653.4	812				
	573	613	538				
	49	129	142				
	35	93	218				
Acer spp.	689	779	407	$R^2 = 0.85$	$R^2 = 0.64$		
	285	296	879				
	291	401	129				
	89	206	442				
	102	80	197				
	62	278	327				
	212	265	300				
	317	298	691				
Aesculus hippocastanum	256	267	289	$R^2 = 0.98$	$R^2 = 0.55$		
	174	173	261				
	837	958	610				
	480	630	444				

shapefile was crucial in defining the specific areas required for mapping the computed CS values [Figs. 2 and 3], focusing solely on the tree species rather than the herbs/shrubs and grasslands.

For validation purposes, 20 plots were considered from a total of 80 as reference points to confirm the results. Out of these 20, 16 were occupied by *Acer spp.* and *Tilia spp.*, while the remaining ones were with the *Aesculus hippocastanum*. A regression analysis was conducted to identify the most accurate relationship between the estimated CS values and the NDVI-derived values obtained through zonal statistics. The best-fitting model was employed to calculate the CS for each species and their respective plots. Later, the R^2 values were generated to illustrate the correlation for each species and the plots.

Pearson's correlation coefficient (r) (i) and the root mean square error (RMSE) (ii) were calibrated to understand the quality of the CS mapping approach concerning the field estimated or Observed CS values (ObsCS) versus the Computed CS values (ComCS) from the validation plots:

$$r = \frac{N(\sum xy) - (\sum x)(\sum y)}{\sqrt{[N\sum x^2 - (\sum x)^2][N\sum y^2 - (\sum y)^2]}} \quad \text{(i)}$$

$$RMSE = \sqrt{\frac{1}{N}\sum_{i=1}^{N}(y - x)^2} \quad \text{(ii)}$$

Where, r= Pearson's correlation coefficient; RMSE= Root Mean Square Error (kg)

x= ComCS (kg); y= ObsCS (kg) and N= number of plots.

3. Results

The computation and visualization of CS for the tree species were conducted based on the tree classification shapefile on QGIS. This mapping approach was done to show the CS distribution across the study area, as depicted in Figs. 2 and 3. The imputed CS values have been illustrated based on the identified species, either in the case of WV3 or Sentinel 2 data. In both cases, except for the leafless or pruned canopies, the CS values using variables derived from NDVI were significant for most of the dominant species. In Fig. 2 and Fig. 3, all three zones (Zoomed in) display a moderate to substantial amount of CS for each species.

In Fig. 2, the calibrated NDVI, even with a coarse resolution, the mapping outcomes have shown the possible tree-stand CS for the identified tree species. The *Acer spp.* and *Aesculus hippocastanum* showed moderate to higher values, whereas the Tilia spp. mostly had lower CS values.

With a better resolution, WV3 data-derived NDVI extracted CS values that were significant for the imputation and mapping of the species-based CS in Brussels [Fig. 3]. Similar areas have been zoomed in to understand and compare the outcomes in both cases for each species.

During the validation, the overall R^2 and Pearson's correlation coefficient r was 0.89 and 0.94 for the WV3 image data, where these values were 0.60 and 0.79, respectively, for the S2 data (Fig. 4, Table 2). Regarding the error analysis, the RMSE, which refers to overall accuracy over all the validation plots, was 189.6 kg for the S2 data, while for the WV3 image data, it was 97 kg (Table 2).

S2 data derived CS per plot for each species were evidently significant, where the R^2 for each species was more than 50 % (Fig. 5). While regarding the WV3 image data, the computed CS per plot was strongly correlated with the estimated CS, showing more than 80 % for each species (Fig. 5).

4. Discussion

A detailed map of species-based CS is essential to establish an efficient urban tree monitoring and management system concerning a

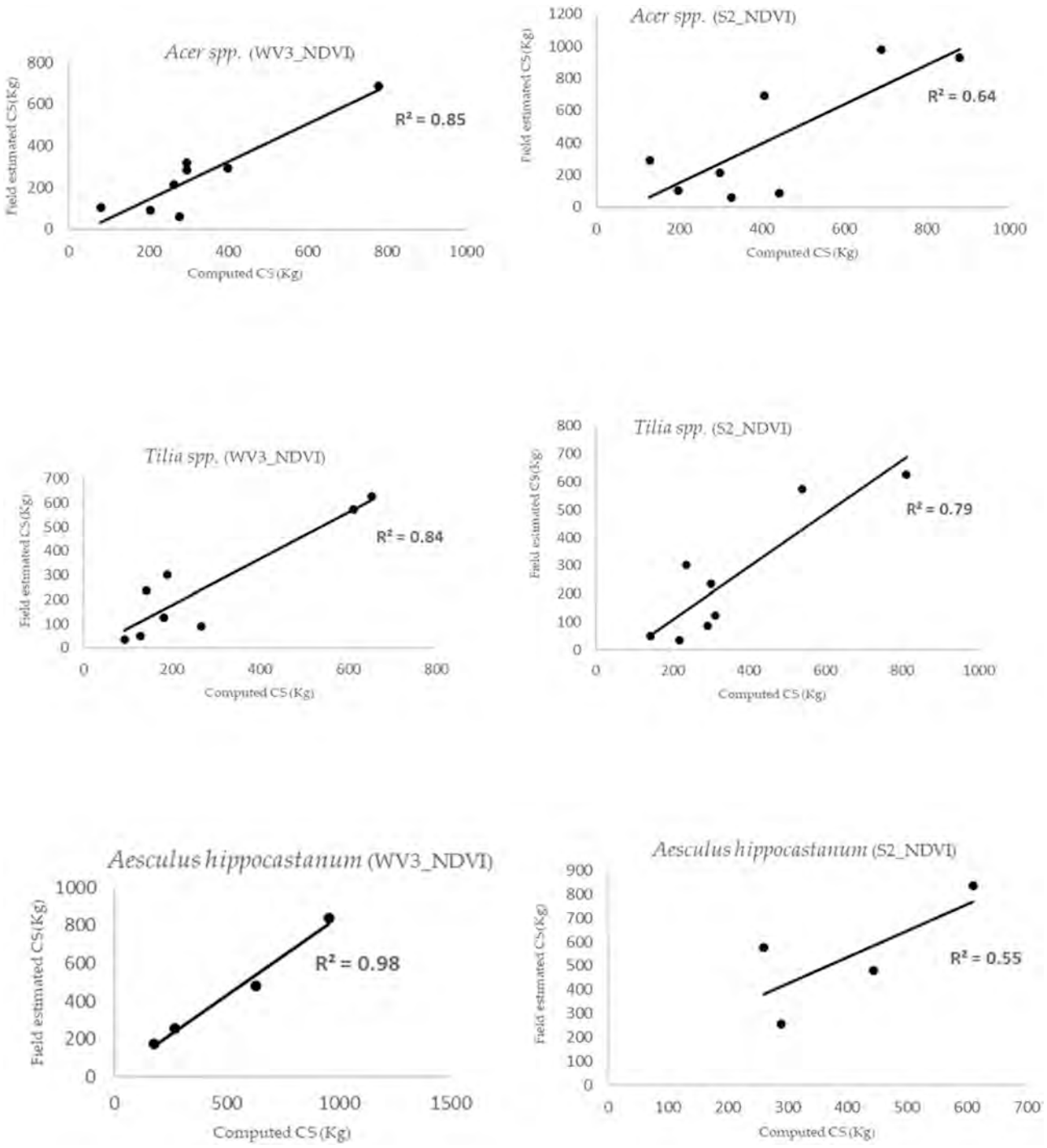

Fig. 5. Correlation among the identified species of the validation plots during the validation.

carbon-neutral city ambient to adapt to the unavoidable effects of climate change. From the late 90 s to the present, many approaches have shown a heightened reliance on remote sensing (RS) technologies (Qin et al., 2022; Vicharnakorn et al., 2014a; Strohbach and Haase, 2012; Yao et al., 2015; Vicharnakorn et al., 2014b; Hutyra et al., 2011; Omasa et al., 2003; Bindu et al., 2020; Jahani and Saffariha, 2022). Yet a convenient method for the city authority, which is easily adaptable concerning the expenses or the availability of remote sensing data, processing skills, or tools, is hardly available. While high-priced data, i.e., LiDAR data, have been widely utilized to improve the accuracy (Calders et al., 2020; Mitchell et al., 2018; Shrestha and Wynne, 2012; Raciti et al., 2014; Alonzo et al., 2016), this study does show strong agreement among the field estimated and imputed CS values (Figs. 4 and 5). The resulting species-based CS imputation has established a strong positive correlation (60 %) with the field estimated values (Fig. 4) even with the Sentinel2 data, while Pearson's r was 0.79 (Table 1). Csillik et al., 2019 proposed a combined Random Forest (RF) machine learning approach (airborne LiDAR data and Planet Dove satellite images) illustrating the $R^2 = 0.70$ (Csillik et al., 2019), while Georgios et al., 2023 reported more than 90 % agreement between the observed and computed values utilizing the terrestrial laser scanning (TLS) (Arseniou et al., 2023). The RMSE for Csillik et al., 2019 was 25.38 Mg C ha−1 while for Georgios et al., 2023, the RMSE was 199 kg calibrated across all over the urban trees (Csillik et al., 2019; Arseniou et al., 2023). This

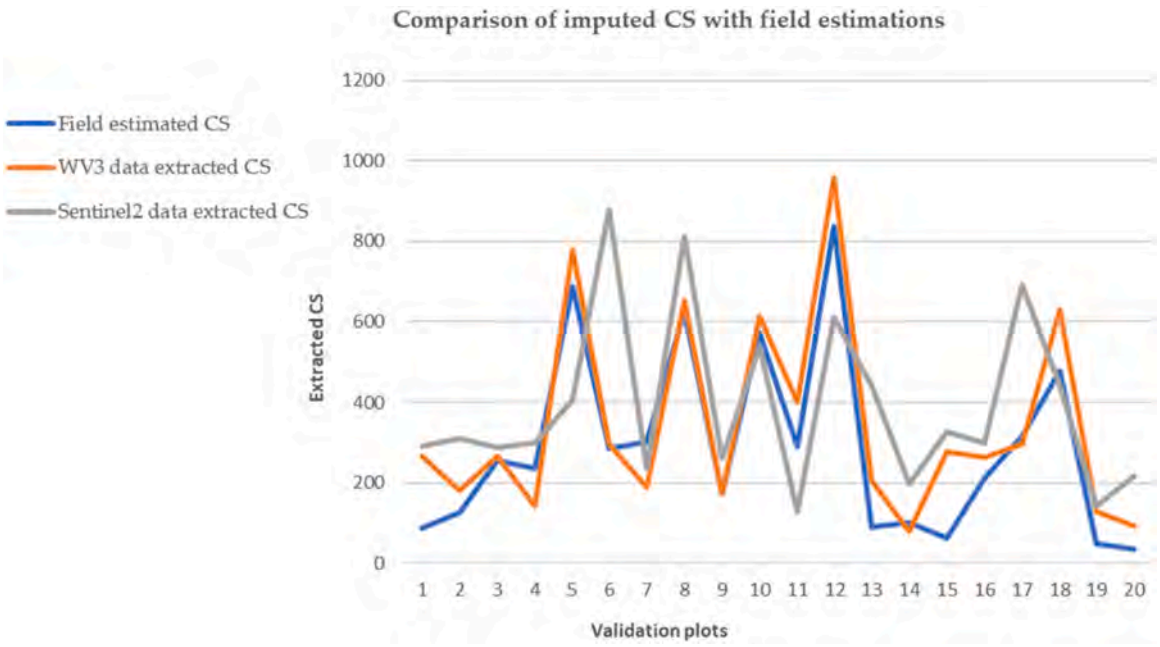

Fig. 6. A line diagram illustrating the correlation among the total CS computations with field estimations.

study shows the RMSE of 189.6 kg for all the validation plots during the CS mapping utilizing the Sentinel2 data, which could be compared with those LiDAR data-based studies. Even in the case of this study, commercial WV3 image data-derived computed CS values have shown a relatively stronger correlation (89 %) with Pearson's r of 0.94 compared with the values derived from the Sentinel2 data. Previous studies have shown lower RMSE, with a Pearson's r/ R^2 of around 0.80 (Jucker et al., 2017; Mascaro et al., 2014; Liang et al., 2016a; Calders et al., 2015; Liang et al., 2016b; Kankare et al., 2013; Stovall et al., 2017).

In contrast, this study shows comparable CS imputation outcomes with Sentinel2 data, where those studies were based on LiDAR data or a combination of LiDAR with other data sources. Concerning the data quality and expenses, this study also illustrates better utilization of WV3 data, which is affordable either in the case of mapping or predicting possible CS for the urban trees (Choudhury et al., 2021, 2020). However, there are a few studies of total AGB/CS estimations where the computations have been done combining the available national tree data with satellite images (Ploton et al., 2020; Cuni-Sanchez et al., 2021; Mugabowindekwe et al., 2023), which could hardly be available with better accuracy, particularly for the complex urban ambient. A methodology could be considered convenient regarding the expenses, but feasibility is also crucial during its application, especially for the public authorities. This study is one of the few available ones where the tree stands CS has been computed and predicted, illustrating a species-specific map for the urban dominant tree species utilizing a free (S2) or comparatively cheaper data (WV3) and at the same time drawing a comparative analysis among the outcomes.

This NDVI-based CS imputation approach could also be easily applied to different smaller study areas (Choudhury et al., 2020). Concerning overall accuracy, especially for the S2 data-derived CS imputations, the higher RMSE (189.6 kg) with a lower agreement (60 %) could be because of the respective NDVI layer. The NDVI layer is well-known for vegetation analysis (Baniya et al., 2018; Atkinson et al., 2012; Pandapotan Situmorang and Sugianto, 2016; Goswami et al., 2015) study also computes CS-based NDVI-extracted metrics. However, NDVI calibration could be affected by cloud contamination, illumination intensity, and sun-target-sensor geometry, which might have unavoidable effects on the pixel-wise parameter outcomes (Hird and McDermid, 2009; Baniya et al., 2018; Van Leeuwen et al., 2013) (Figs. 2 and 3). For instance, for a few plots (7 and 17), S2 data extracted CS showed more significant (Fig. 6) differences than those for the case of the WV3 data. This is clearly because of the top-of-atmosphere (TOA) NDVI reduction, which is highly responsible for misinterpretation of the vegetation information due to the clouds (Hird and McDermid, 2009; Chen et al., 2004; Yang et al., 2019). For the WV3 data, the effects were way less, resulting in the mapping outcomes way better than the Sentinel2 data. A precise and accurate urban tree classification map is essential for appropriate species-based mapping, which could be a challenge for city planners. The details about the tree species classification and identification approach have been discussed in previous studies (Choudhury et al., 2021, 2020), which could be easily adapted, especially for the complex urban landscape and green space classification, for a better management and monitoring system. Also, previously it has been shown that the LiDAR data could cost a lot (USD 62–240 perkm^2) (Choudhury et al., 2021; Ørka and Hauglin, 2016; Wang et al., 2018), WV3 image data is comparatively cheaper (USD 19 perkm^2) (Choudhury et al., 2021) concerning the tree species-based mapping and imputations. This study shows the efficiency and potential of the Sentinel2 data, which is freely available and accessible from anywhere all over the planet. Moreover, this Copernicus free data is being updated, acquiring images every five days (Shafizadeh-Moghadam et al., 2022; Cai et al., 2019; Castaldi et al., 2019; Zhou et al., 2020), which could be an additional benefit for ensuring a continuous urban monitoring system. Most European cities have the updated tree data (https,https,https,https,kartta, https); this study could be a solid prospect to go through an efficient urban green monitoring and management system utilizing the S2 data.

A sustainable urban tree monitoring and management system corresponds to the goal of carbon offsetting through afforestation or reforestation, which hugely depends on the potential evaluation of the existing dominant species. This study could be an initiative to adopt an efficient monitoring system for the city authorities towards achieving the goal of net-zero carbon emission. While cities worldwide are increasingly adopting carbon-neutral plans insisting on ensuring the maximum utilization of green spaces (Solano et al., 2021), this study on Brussels could be an essential addition to the strategies for policymakers. Concerning convenience, this approach could be tested for developing countries where remote sensing data access and processing is hardly convenient.

5. Conclusions

The carbon capture and storage potentiality of trees and their beneficial impacts on an urban environment have been continuously explored for the last few decades. Regarding approaches concerning urban trees, it is always sprawled with several issues due to the complex city agglomeration. That is why different remote-sensing methods are utilized where high-priced data, skills, and expenses regarding their processing and applications hugely limit the severe adaptations for different situations. This study illustrates CS imputations by potentially mapping species-specific outcomes by comparing two other data sources. Certainly, coarse resolution, along with NDVI computations, will have unavoidable limitations, but it is essential to consider the prospects concerning the possibility of adaptations or availability for the public authorities. This approach does require going through a few more assessments, especially for developing countries, where carbon-neutral or climate-friendly environments towards carbon offsetting through urban trees should be introduced as an efficient solution to combat the extremity of the relentless effects of global warming. Nevertheless, this study also shows lower differences concerning the error (RMSE 97 kg and 189.6 kg) and a strong correlation with the imputed CS values (89 % and 60 %), which could be comparable to the findings based on the approaches with the high-priced data sources. It could be essential to recommend a possible way out concerning an adaptive urban tree planning and monitoring system toward a carbon-neutral city environment for the city authorities.

Funding

This research received no external funding.

CRediT authorship contribution statement

MD Abdul Mueed Choudhury: Writing – review & editing, Writing – original draft, Visualization, Validation, Software, Methodology, Investigation, Formal analysis, Data curation, Conceptualization. **Ernesto Marcheggiani:** Writing – review & editing, Writing – original draft, Supervision, Methodology, Conceptualization. **Giuseppe Modica:** Writing – review & editing, Writing – original draft, Visualization, Supervision, Resources, Methodology, Conceptualization. **Salvatore Praticò:** Visualization, Resources, Data curation. **Ben Somers:** Writing – review & editing, Writing – original draft, Supervision, Resources, Conceptualization.

Declaration of Competing Interest

The authors declare that they have no known competing financial interests or personal relationships that could have appeared to influence the work reported in this paper.

References

Lechtenböhmer, S., et al., 2009. Sustainable Urban Infrastructure. Munich Ed. ; paths a Carbon-Free Future.

OPUS 4 | Sustainable Urban Infrastructure: Munich edition; paths toward a carbon-free future. https://epub.wupperinst.org/frontdoor/index/index/docId/3331.

Kanniah, K.D., Muhamad, N., CS, K., 2014. Remote sensing assessment of carbon storage by urban forest. InIOP Conf. Ser.: Earth Environ. Sci. *Vol.* 18, 1.

Rosenfeld, A.H., Akbari, H., Romm, J.J., Pomerantz, M., 1998. Cool communities: Strategies for heat island mitigation and smog reduction. Energy Build. 28, 51–62.

Sahle, M., Saito, O., Fürst, C., Yeshitela, K., 2018. Quantification and mapping of the supply of and demand for carbon storage and sequestration service in woody biomass and soil to mitigate climate change in the socio-ecological environment. Sci. Total Environ. 624, 342–354.

Gülçin, D., Konijnendijk Van Den Bosch, C.C., 2021. Assessment of above-ground carbon storage by urban trees using lidar data: The case of a university campus. Forests 12, 1–20.

Qin, H., Zhou, W., Qian, Y., Zhang, H., Yao, Y., 2022. Estimating aboveground carbon stocks of urban trees by synergizing ICESat-2 LiDAR with GF-2 data. Urban Urban Green. 76, 127728.

Choudhury, M.A.M., Marcheggiani, E., Galli, A., Modica, G., Somers, B., 2021. Mapping the Urban Atmospheric Carbon Stock by LiDAR and WorldView-3 Data. For. 2021, Vol. 12, Page 692 12, 692.

Choudhury, M.A.M., et al., 2020. Urban Tree Species Identification and Carbon Stock Mapping for Urban Green Planning and Management. Forests 11, 1226.

Li, X., Chen, W.Y., Sanesi, G., Lafortezza, R., 2019. Remote Sensing in Urban Forestry: Recent Applications and Future Directions. Remote Sens 11, 1144.

Song, Y., Imanishi, J., Sasaki, T., Ioki, K., Morimoto, Y., 2016. Estimation of broad-leaved canopy growth in the urban forested area using multi-temporal airborne LiDAR datasets. Urban 16, 142–149.

Myeong, S., Nowak, D.J., Duggin, M.J.A., 2006. temporal analysis of urban forest carbon storage using remote sensing. Remote Sens 101, 277–282.

Feng, S., et al., 2016. Los Angeles megacity: a high-resolution land–atmosphere modelling system for urban CO2 emissions. Atmos. Chem. Phys. 16, 9019–9045.

Wei, D., Reinmann, A., Schiferl, L.D., Commane, R., 2022. High resolution modeling of vegetation reveals large summertime biogenic CO2 fluxes in New York City. Environ. Res. Lett. 17, 124031.

Wilkes, P., Disney, M., Vicari, M.B., Calders, K., Burt, A., 2018. Estimating urban above ground biomass with multi-scale LiDAR. Carbon Balance Manag 13, 10.

Mariappan, M., et al., 2012. Carbon accounting of urban forest in Chennai City using Lidar data. Eur. J. Sci. Res 81, 314–328.

Zhang, Y., Shao, Z., 2021. Assessing of Urban Vegetation Biomass in Combination with LiDAR and High-resolution Remote Sensing Images. Int J. Remote Sens 42, 964–985.

Pu, R.L., 2011. Mapping urban forest tree species using IKONOS imagery: Preliminary results. Environ. Monit. Assess. 172, 199–214.

Tigges, J., Lakes, T., 2017. High resolution remote sensing for reducing uncertainties in urban forest carbon offset life cycle assessments. Carbon Balance Manag 12.

Panagiotidis, D., Surový, P., Kuželka, K., 2016a. Accuracy of Structure from Motion models in comparison with terrestrial laser scanner for the analysis of DBH and height influence on error behaviour. J. Sci. (Prague) 62, 357–365.

Yao, W., Krzystek, P., Heurich, M., 2012. Tree species classification and estimation of stem volume and DBH based on single tree extraction by exploiting airborne full-waveform LiDAR data. Remote Sens Environ. 123, 368–380.

Panagiotidis, D., Surový, P., Kuželka, K., 2016b. Accuracy of Structure from Motion models in comparison with terrestrial laser scanner for the analysis of DBH and height influence on error behaviour. J 62, 357–365.

Mitchell, M.G.E., et al., 2018. Identification of fine scale and landscape scale drivers of urban aboveground carbon stocks using high-resolution modeling and mapping. Sci. Total Environ. 622, 57–70.

Shrestha, R., Wynne, R.H., 2012. Estimating Biophysical Parameters of Individual Trees in an Urban Environment Using Small Footprint Discrete-Return Imaging Lidar. Remote Sens (Basel) 4, 484–508.

Raciti, S.M., Hutyra, L.R., Newell, J.D., 2014. Mapping carbon storage in urban trees with multi-source remote sensing data: Relationships between biomass, land use, and demographics in Boston neighborhoods. *Sci. Total Environ.* 500–501 72–83.

Alonzo, M., McFadden, J.P., Nowak, D.J., Roberts, D.A., 2016. Mapping urban forest structure and function using hyperspectral imagery and lidar data. Urban Urban Green. 17, 135–147.

He, S., et al., 2020. Intelligent Mapping of Urban Forests from High-Resolution Remotely Sensed Imagery Using Object-Based U-Net-DenseNet-Coupled Network. Remote Sens (Basel) 12, 3928.

Fassnacht, F.E., et al., 2016. Review of studies on tree species classification from remotely sensed data (Preprint at). Remote Sens. Environ. vol. 186, 64–87. https://doi.org/10.1016/j.rse.2016.08.013 (Preprint at).

Johnson, B., Jozdani, S., 2018. Identifying Generalizable Image Segmentation Parameters for Urban Land Cover Mapping through Meta-Analysis and Regression Tree Modeling. Remote Sens (Basel) 10, 73.

Degerickx, J., Hermy, M., Somers, B., 2020. Mapping Functional Urban Green Types Using High Resolution Remote Sensing Data. Sustainability 12, 2144.

Puissant, A., Rougiera, S., Stumpf, A., 2014. Object-oriented mapping of urban trees using random forestclassifiers. Int. J. Appl. Earth Obs. Geoinf. 26, 235–245.

Pu, R., Landry, S., 2020. Mapping urban tree species by integrating multi-seasonal high resolution pléiades satellite imagery with airborne LiDAR data. Urban Urban Green. 53, 126675.

Pu, R., Landry, S., 2012. A comparative analysis of high spatial resolution IKONOS and WorldView-2 imagery for mapping urban tree species. Remote Sens Environ. 124, 516–533.

Solano, F., Di Fazio, S., Modica, G., 2019. A methodology based on GEOBIA and WorldView-3 imagery to derive vegetation indices at tree crown detail in olive orchards. Int. J. Appl. Earth Obs. Geoinf. 83, 101912.

Tabacchi, G., Cosmo, D., Gasparini, L., 2011a. & tree volume, P. A. and phytomass prediction equations for forest species in Italy. Eur. J. For. Res 130, 911–934.

Congedo Luca. The Semi-Automatic Classification Plugin (SCP)-QGIS Python Plugins Repository. https://plugins.qgis.org/plugins/SemiAutomaticClassificationPlugin/.

Nikon | News | Nikon Introduces New Laser Rangefinder 'Forestry 550'. https://www.nikon.com/news/2008/0924_forestry_02.htm.

Tabacchi, G., Di Cosmo, L., Gasparini, P., 2011b. Aboveground tree volume and phytomass prediction equations for forest species in Italy. Eur. J. For. Res (2011) *130, 911–934.* https://doi.org/10.1007/s10342-011-0481-9.

Goslee, K., et al., 2010. Leaf Technicial Guidance Series for the development of a forest carbon monitoring system for REDD+: Module C-CS. Calc. Estim. Carbon Stocks.

1986 biomass, B. S. E. and biomass change of tropical forests: a primer. Rome: FAO For. Pap. 134, 1986.

Losi, C.J., Siccama, T.G., Condit, R., JE, M., 2003. Analysis of alternative methods for estimating carbon stock in young tropical plantatiions. Ecol. Manag. 355–368.

Vashum, K.T., Jayakumar, S., 2012. Methods to estimate above-ground biomass and carbon stock in natural forests-a review. J. Ecosyst. Ecography 2, 1–7.
Whittaker, R.H. & GE, L.. Carbon in the biota. in Woodwell GM, Pecan EV, Carbon in the biosphere, Proceedings of the 24th Brookhaven Symposium in biology. Upton,: United States Atomic Energy Commission,*1973*,. [CrossRef] 281–302.
Statistics, F.A.O., 2010. Food and Agriculture Organization of the United Nations. Retrieved 3, 2012.
Vicharnakorn, P., Shrestha, R.P., Nagai, M., Salam, A.P., Kiratiprayoon, S., 2014a. Carbon stock assessment using remote sensing and forest inventory data in Savannakhet, Lao PDR. Remote Sens. 6, 5452–5479.
Panel, I., 2007. On Climate Change (IPCC). (Cambridge University Press, Cambridge.
Congedo, L., 2016. Semi-automatic classification plugin documentation. Release 4, 29.
Congedo, L., 2021. Semi-Automatic Classification Plugin: A Python tool for the download and processing of remote sensing images in QGIS. J. Open Source Softw. 6, 3172.
Shafizadeh-Moghadam, H., Minaei, F., Talebi-khiyavi, H., Xu, T., Homaee, M., 2022. Synergetic use of multi-temporal Sentinel-1, Sentinel-2, NDVI, and topographic factors for estimating soil organic carbon. Catena (Amst.) 212, 106077.
Hird, J.N., McDermid, G.J., 2009. Noise reduction of NDVI time series: an empirical comparison of selected techniques. Remote Sens Environ. 113, 248–258.
Baniya, B., Tang, Q., Huang, Z., Sun, S., Techato, K., 2018. Spatial and Temporal Variation of NDVI in Response to Climate Change and the Implication for Carbon Dynamics in Nepal. Forests 9, 329.
Jung, M., 2013. LecoS-A QGIS Plugin Autom. Landsc. Ecol. Anal.
AG, D.. *ECognition Version 5 Object Oriented Image Analysis User Guide*. 2005. (Munich, Germany).
Strohbach, M., Haase, D., 2012. The above-ground carbon stock of a central European city: patterns of carbon storage in trees in Leipzig, Germany. Land. Urban Plan 104, 95–104.
Yao, Z.Y., Liu, J.J., Zhao, X.W., Long, D.F., Wang, L., 2015. Spatial dynamics of aboveground carbon stock in urban green space: a case study of Xi'an, China. J. Arid Land 7, 350–360.
Vicharnakorn, P., Shrestha, R., Nagai, M., Salam, A., Kiratiprayoon, S., 2014b. Carbon Stock Assessment Using Remote Sensing and Forest Inventory Data in Savannakhet, Lao PDR. Remote Sens (Basel) 6, 5452–5479.
Hutyra, L.R., Yoon, B., Alberti, M., 2011. Terrestrial carbon stocks across a gradient of urbanization: A study of the Seattle, WA region. Glob. Chang Biol. 17, 783–797.
Omasa, K., Qiu, G.Y., Watanuki, K., Yoshimi, K., Akiyama, Y., 2003. Accurate estimation of forest carbon stocks by 3-D remote sensing of individual trees. Environ. Sci. Technol. 37, 1198–1201.
Bindu, G., Rajan, P., Jishnu, E.S., Ajith Joseph, K., 2020. Carbon stock assessment of mangroves using remote sensing and geographic information system. Egypt. J. Remote Sens. Space Sci. 23, 1–9.
Jahani, A., Saffariha, M., 2022. Environmental decision support system for Plane trees failure prediction: A comparison of multi-layer perceptron and random forest modeling approaches. Agrosystems, Geosci. Environ. 5, e20316.
Calders, K., et al., 2020. Terrestrial laser scanning in forest ecology: Expanding the horizon. Remote Sens Environ. 251, 112102.
Csillik, O., Kumar, P., Mascaro, J., O'Shea, T., Asner, G.P., 2019. Monitoring tropical forest carbon stocks and emissions using Planet satellite data (Preprint at). Sci. Rep. 9, 17831 (Preprint at).
Arseniou, G., MacFarlane, D.W., Calders, K., Baker, M., 2023. Accuracy differences in aboveground woody biomass estimation with terrestrial laser scanning for trees in urban and rural forests and different leaf conditions. Trees 1–19.
Jucker, T., et al., 2017. Allometric equations for integrating remote sensing imagery into forest monitoring programmes. Glob. Chang Biol. 23, 177–190.
Mascaro, J., et al., 2014. A tale of two "forests": Random Forest machine learning aids tropical forest carbon mapping. PLoS One 9, e85993.
Liang, X., et al., 2016a. Terrestrial laser scanning in forest inventories. ISPRS J. Photogramm. Remote Sens. 115, 63–77.
Calders, K., et al., 2015. Nondestructive estimates of above-ground biomass using terrestrial laser scanning. Methods Ecol. Evol. 6, 198–208.
Liang, X., et al., 2016b. Terrestrial laser scanning in forest inventories. ISPRS J. Photogramm. Remote Sens. 115, 63–77.
Kankare, V., et al., 2013. Individual tree biomass estimation using terrestrial laser scanning. ISPRS J. Photogramm. Remote Sens. 75, 64–75.
Stovall, A.E.L., Vorster, A.G., Anderson, R.S., Evangelista, P.H., Shugart, H.H., 2017. Non-destructive aboveground biomass estimation of coniferous trees using terrestrial LiDAR. Remote Sens Environ. 200, 31–42.
Ploton, P., et al., 2020. A map of African humid tropical forest aboveground biomass derived from management inventories. Sci. Data 7, 221.
Cuni-Sanchez, A., et al., 2021. High aboveground carbon stock of African tropical montane forests. Nature 596, 536–542.
Mugabowindekwe, M., et al., 2023. Nation-wide mapping of tree-level aboveground carbon stocks in Rwanda. Nat. Clim. Chang 13, 91–97.
Atkinson, P.M., Jeganathan, C., Dash, J., Atzberger, C., 2012. Inter-comparison of four models for smoothing satellite sensor time-series data to estimate vegetation phenology. Remote Sens Environ. 123, 400–417.
Pandapotan Situmorang, J., Sugianto, S., 2016. Estimation of Carbon Stock Stands using EVI and NDVI vegetation index in production forest of lembah Seulawah sub-district, Aceh Indonesia. Aceh Int. J. Sci. Technol. 5, 126–139.
Goswami, S., Gamon, J., Vargas, S., 2015. & of Ndvi, T. C. R. Biomass, and Leaf Area Index (LAI) for six key plant species in Barrow, Alaska. PeerJ Prepr. ;Mar. 19.
Van Leeuwen, W.J.D., Hartfield, K., Miranda, M., Meza, F.J., 2013. Trends and ENSO/AAO driven variability in NDVI derived productivity and phenology alongside the Andes Mountains. Remote Sens (Basel) 5, 1177–1203.
Chen, J., et al., 2004. A simple method for reconstructing a high-quality NDVI time-series data set based on the Savitzky–Golay filter. Remote Sens Environ. 91, 332–344.
Yang, Y., Luo, J., Huang, Q., Wu, W., Sun, Y., 2019. Weighted double-logistic function fitting method for reconstructing the high-quality sentinel-2 NDVI time series data set. Remote Sens (Basel) 11, 2342.
Ørka, H.O. & Hauglin, M. Use of remote sensing for mapping of non-native conifer species. *76* (2016).
Wang, K., Wang, T., Liu, X., 2018. A review: Individual tree species classification using integrated airborne LiDAR and optical imagery with a focus on the urban environment. Forests 10, 1.
Cai, Y., Lin, H., Zhang, M., 2019. Mapping paddy rice by the object-based random forest method using time series Sentinel-1/Sentinel-2 data. Adv. Space Res. 64, 2233–2244.
Castaldi, F., et al., 2019. Evaluating the capability of the Sentinel 2 data for soil organic carbon prediction in croplands. ISPRS J. Photogramm. Remote Sens. 147, 267–282.
Zhou, T., et al., 2020. High-resolution digital mapping of soil organic carbon and soil total nitrogen using DEM derivatives, Sentinel-1 and Sentinel-2 data based on machine learning algorithms. Sci. Total Environ. 729, 138244.
https⟨://www.wien.gv.at/stadtgruen/parks/baumkataster/⟩.
https⟨://baumkataster.berlin.de/⟩.
https⟨://data.london.gov.uk/dataset/gla-trees⟩.
https⟨://bomen.amsterdam.nl/⟩.
kartta.hel.fi/urbanforest.
https⟨://www.paris.fr/inventaire-des-arbres-parisiens-2260⟩.
Solano, F., et al., 2021. Characterizing historical transformation trajectories of the forest landscape in Rome's metropolitan area (Italy) for effective planning of sustainability goals. Land Degrad. Dev. 32, 4708–4726.